Mechanism of K^+-induced Actin Assembly

JOEL D. PARDEE and JAMES A. SPUDICH
Department of Structural Biology, Sherman Fairchild Center, Stanford University School of Medicine, Stanford, California 94305

ABSTRACT The assembly of highly purified actin from *Dictyostelium discoideum* amoebae and rabbit skeletal muscle by physiological concentrations of KCl proceeds through successive stages of (*a*) rapid formation of a distinct monomeric species referred to as KCl-monomer, (*b*) incorporation of KCl-monomers into an ATP-containing filament, and (*c*) ATP hydrolysis that occurs significantly after the incorporation event. KCl-monomer has a conformation which is distinct from that of either conventional G- or F-actin, as judged by UV spectroscopy at 210–220 nm and by changes in ATP affinity. ATP is not hydrolyzed during conversion of G-actin to KCl-monomer. KCl-monomer formation precedes filament formation and may be necessary for the assembly event. Although incorporation of KCl-monomers into filaments demonstrates lag-phase kinetics by viscometry, both continuous absorbance monitoring at 232 nm and rapid sedimentation of filaments demonstrate hyperbolic assembly curves. ATP hydrolysis significantly lags the formation of actin filaments. When half of the actin has assembled, only 0.1 to 0.2 mole of ATP are hydrolyzed per mole of actin present as filaments.

The biochemical mechanisms that govern the intracellular equilibrium position of monomeric and filamentous actin remain largely unknown. Early observations of the array of actin filaments within striated muscle myofibrils led to the supposition that actin exists almost totally in the filamentous form under intracellular conditions. However, with the discovery that large amounts of monomeric actin exist in extracts of nonmuscle cells (5, 17) there is renewed interest in understanding the biochemical signals that modulate the G ↔ F assembly process.

Polymerization of G-actin is thought to occur as a result of partial neutralization of surface charge by cations present as neutral salts in the assembly buffer (1, 2, 15, 19, 21, 22, 28). Two studies have directly reported on charge reduction of actin by divalent cations during polymerization (18, 29). However, the mechanism of actin assembly by monovalent cations has not been elucidated, although K^+ has long been known to induce assembly of actin at approximately 100-fold higher concentrations than required for divalent cations. The importance of clearly defining the mechanism of K^+-induced assembly becomes apparent in terms of understanding assembly controls operative in vivo, when one considers the high concentration of K^+ (100 mM range) (8, 11) constantly bathing intracellular actin.

Conformational differences between F- and G-actins have been directly observed by UV difference spectra (10) with the F-actin conformation characterized by absorbance maxima at 232 nm and 290 nm. Rich and Estes (23) subsequently obtained evidence for conformational changes in actin by comparing initial rates of proteolytic digestion. Their results showed that G-actin in the absence of KCl is hydrolyzed at a four- to sixfold greater rate than F-actin assembled by 0.1 M KCl. Moreover, addition of 0.1 M KCl to G-actin at a concentration below that required to allow assembly (C_A) resulted in the formation of a species called F-monomer exhibiting the lower susceptibility to proteolysis typical of F-actin (23). Recently, Rouayrenc and Travers (24) have directly detected the formation of F-monomer (or G*-actin) by UV difference spectra in the range 250–300 nm. They were able to detect a maximum change in absorbance at 275 nm when the temperature was lowered to 4°C to raise the apparent C_A to 500 μg/ml in 0.1 M KCl and 0.1 mM $CaCl_2$.

Since intracellular actin is constantly exposed to high K^+ concentrations (8, 11), we wished to study the effect of K^+ on the full assembly process of actin isolated from both rabbit skeletal muscle and *Dictyostelium discoideum* amoebae. Through these studies, it has been possible to more completely analyze the sequence of events leading to the formation of actin filaments.

MATERIALS AND METHODS

Actin Isolation

Rabbit skeletal muscle actin was purified by the method of Spudich and Watt (27). *Dictyostelium* actin was isolated by the procedure of Uyemura, et al. (32). Isolated F-actins (4–6 mg/ml) were subsequently depolymerized by dialysis against 1 liter of 2 mM triethanolamine, pH 7.4, 0.1 mM ATP, 0.5 mM 2-

THE JOURNAL OF CELL BIOLOGY · VOLUME 93 JUNE 1982 648-654

mercaptoethanol, 0.005% NaN_3 at 4°C for 24 h in 10,000-dalton cutoff collodion bags (Schleicher & Schull, Inc., Keene, NH). Homogeneous populations of G-actin monomers for both spectroscopy and assembly experiments were obtained by chromatography of depolymerized actin at 4°C through a 2 X 60-cm column of G-150 Sephadex (Pharmacia, Uppsala, Sweden) pre-equilibrated in the experimental buffer of choice. The column was calibrated with ribonuclease A, ovalbumin, bovine serum albumin, and Blue Dextran 2000 (Pharmacia, Uppsala, Sweden). For UV difference spectroscopy, monomers were eluted in 1 mM TES, pH 7.4, 25 μm ATP, 0.1 mM 2-mercaptoethanol (Buffer I), whereas for assembly experiments, monomers were eluted in 5 mM triethanolamine, pH 7.4, 0.1 mM ATP, 0.5 mM 2-mercaptoethanol, 0.005% NaN_3 (Buffer II). Actin monomers were used immediately after elution from the G-150 Sephadex column.

UV Difference Spectroscopy

Actin monomers were pooled from the G-150 Sephadex column in Buffer I and diluted to the appropriate concentration (10–100 μg/ml) with column-equilibrated buffer. Difference spectra were obtained at 25°C in either a Beckman 35 (Beckman Instruments, Palo Alto, CA) or Cary 118 (Varian, Palo Alto, CA) dual beam scanning spectrophotometer. Divided Spectracil quartz cuvettes of 0.4 cm pathlength per well (Precision Cell, Hicksville, NY) were used; the two wells are in series with respect to the beam. An aliquot of actin monomer (0.80 ml) was pipetted into one well of the sample and reference cuvettes, and an equal volume of column-equilibrated Buffer I was placed into the tandem well of each cuvette. Actin concentrations of ≤50 μg/ml were used to prevent filament formation. Previous experiments using viscometry and ΔOD_{232} measurements established that the critical actin concentration required for actin assembly by 0.1 M KCl in this buffer was 50 μg/ml (data not shown). Baseline spectra of G-actin versus G-actin were taken from 400 nm to 200 nm. To obtain difference spectra of KCl-monomer, 88 μl of 1.0 M KCl stock solution (in Buffer I) was added directly to the actin well of the sample beam cuvette and to the buffer well of the reference cuvette. Equal volumes of buffer were added to the opposite wells, the samples mixed with a teflon rod, and spectra taken at 30-min intervals from 400 to 200 nm over a period of several hours. To optimize instrument signal-to-noise ratio at the shorter wavelengths (<230 nm), a "wide" slit program, 1.0-mm aperture, 2-s pen period, and a scanning speed of 25 nm per minute were used. High buffer absorbance from 260 nm to 200 nm was greatly reduced by using TES buffer, an ATP concentration of 25 μM, and 2-mercaptoethanol rather than dithiothreitol. Since G-actin was shown to have an affinity for ATP of $K_a \approx 5 \times 10^6\ M^{-1}$ (see Fig. 6 of Results), equilibration of G-actin with 25 μm ATP provided >98% saturation of actin monomer with nucleotide. Assembly of KCl-monomers into filaments and spectral evidence for the conversion of KCl-monomers into F-actin was obtained by two methods. After recording a KCl-monomer spectrum, 1 mM $MgCl_2$ was added to the actin well and buffer wells of the sample and reference cuvettes, respectively, and spectra were taken at various times after Mg^{2+} addition. In the buffer used, both rabbit skeletal muscle and *Dictyostelium* actin critical concentrations (C_A) drop from 50 μg/ml to <10 μg/ml upon addition of Mg^{2+} and assembly is initiated. In a second method G-actin at greater than C_A was placed in cuvettes, 0.1 M K^+ added, and spectra were taken during assembly at 25°C. The unassembled G-actin in the reference beam cuvette was examined for light scattering at 320 nm after termination of difference spectral analysis, and the assembled actin in the sample cuvette was subjected to viscometry to determine the extent of polymerization. Absorbance differences obtained in 0.4 cm divided cuvettes were normalized to a 1.0-cm path length, subtracted from the G-actin vs. G-actin baseline, and plotted.

Spectroscopic Titration of G-actin with KCl

K^+ saturation curves for G-actin at 25°C were obtained spectroscopically at 215 and 220 nm. Monomeric G-actin (0.80 ml, 45 μg/ml) in Buffer I was placed in divided cuvettes with Buffer I in the opposite wells. KCl stock (3.0 M) was added to final concentrations of from 2 mM to 0.3 M, and the absorbance recorded after each addition. Absorbance differences were corrected for dilution of actin by KCl stock, normalized to a 1-cm cuvette path length, and plotted against KCl concentration. The titrated actin sample (at 0.3 M KCl) was tested for the presence of assembled actin by viscometry in a Cannon-Manning capillary viscometer (Cannon Instrument Co., State College, PA) and by absorbance at 232 nm.

ATP Binding to G-actin and KCl-monomer

The affinity of ATP for G-actin and KCl-monomer was analyzed by equilibrium dialysis at 4°C. G-actin monomer was eluted from G-150 Sephadex in 5 mM triethanolamine, pH 7.4, 0.5 mM 2-mercaptoethanol, 20 μM ATP and 0.005% NaN_3 (Buffer III), diluted to 50 μg/ml, and freshly prepared [γ-^{32}P]-ATP (13 Ci/mmol; reference 6) added to a final concentration of 1 μM. After incubation for 1 h on ice, 200-μl aliquots of labeled sample were pipetted into 10,000-dalton cutoff collodion bags which had been pre-equilibrated with cold buffer. Samples were rapidly dialyzed at 4°C against various volumes of Buffer III containing no ATP. Buffer volumes were calculated to achieve final ATP concentrations ranging from 0.1 to 4 μM. Aliquots (5 μl) from inside and outside the bag were counted at 30-min intervals to monitor approach to equilibrium of the sample with buffer. Complete equilibration was obtained after 8–10 h of dialysis. Upon reaching equilibrium, aliquots were removed from both inside and outside the bag and assayed for the concentrations of actin, inorganic phosphate (P_i) resulting from ATP hydrolysis, free ATP, and actin-bound ATP. Four 10-μl aliquots from both inside and outside the bag were counted in 5 ml of Aquascint (Calbiochem, La Jolla, CA), and bound ATP was determined after subtraction of counts due to $^{32}P_i$. Duplicate 10-μl aliquots from inside and outside the bag were assayed for $^{32}P_i$ by an adaptation of the method of Sugino and Miyoshi (7, 30). Actin concentration after dialysis was determined from absorbance of the actin sample at 280 and 290 nm using the extinction coefficients $\epsilon_{280}^{0.1\%} = 1.108\ cm^{-1}$ (33) and $\epsilon_{290}^{0.1\%} = 0.62\ cm^{-1}$ (12), respectively. Affinity constants and moles ATP bound per mole actin were obtained by Scatchard analysis (25).

Control experiments without actin demonstrated that [γ-^{32}P]-ATP was completely equilibrated across collodion bags in Buffer III within 6–8 h at 4°C. Equilibration of ATP is difficult to achieve with conventional dialysis membranes under these low ionic strength conditions.

The ability of dialyzed actin samples to assemble was measured and only those samples demonstrating >90% assembly competency were used in binding determinations. Actin remaining inside the collodion bag after removal of all assay aliquots was incubated on ice with 1.0 mM ATP overnight. The mixture was brought to room temperature, 0.1 M KCl and 1.0 mM $MgCl_2$ were added and assembly monitored at 232 nm (10). The assembly competency of the actin was taken as evidence of nucleotide binding to a nondenatured actin conformation.

Identical procedures were used to determine ATP affinity to KCl-monomer actin, except that 0.1 M KCl was added to the dialyzing buffer and actin sample just before equilibrium dialysis.

Assembly Kinetics

For simultaneous measurements of assembly by ΔOD_{232}, ATPase assays, viscometry, and sedimentation, *Dictyostelium* and rabbit skeletal muscle actins (at 0.5 mg/ml, eluted from G-150 Sephadex in Buffer II) were labeled with 0.5 μM freshly chromatographed [γ-^{32}P]-ATP (6 Ci/mmol) by incubation for 1 h on ice. Control experiments showed maximal exchange of label into actin within 30 min at 0°C with negligible hydrolysis of [γ-^{32}P]-ATP.

For ΔOD_{232} measurements G-actin (0.5 mg/ml) was pipetted into a 1 cm pathlength quartz cuvette, 0.1 M KCl or 0.1 M KCl plus 0.2 mM $MgCl_2$ mixed in from stock solutions, and assembly continuously monitored at 232 nm against a buffer reference in a Beckman 35 spectrophotometer (Beckman Instruments, Inc.). A second salt-free G-actin sample was incubated at 25°C during assembly and subsequently monitored at 232 nm for absorbance changes due to light scattering. No corrections for light scatter were necessary.

Hydrolysis of [γ-^{32}P]-ATP during the course of assembly was determined by the modified method of Sugino and Miyoshi (30) described in detail elsewhere (7). Hydrolysis was determined on actin samples being monitored simultaneously for assembly by ΔOD_{232}. 5-μl aliquots were removed directly from the cuvette and hydrolysis stopped with 0.9 ml cold 0.15 M perchloric acid in 2×10^{-5} M potassium phosphate (7). Control experiments with either G-actin in Buffer II or Buffer II containing 0.1 M KCl, 0.2 mM $MgCl_2$ in the absence of actin demonstrated no measurable ATP hydrolysis. The amount of ATP hydrolyzed per mole actin was calculated from the F-actin concentration after assembly and from the specific activity of total ATP present after addition of label. Under these salt conditions, actin is >90% assembled by 0.1 M KCl and >98% assembled by 0.1 M KCl + 0.2 mM $MgCl_2$ ($C_A = 50$ μg/ml in 0.1 M KCl; $C_A < 10$ μg/ml in 0.1 M KCl, 0.2 mM $MgCl_2$).

Viscosity measurements were performed in a Cannon-Manning 100 capillary viscometer with a buffer outflow time of 62 s at 25°C. Viscometry was performed in parallel with ΔOD_{232}, ATPase, and sedimentation assays using identical aliquots of G-actin in Buffer II.

Assembly of actin was also followed by rapid sedimentation. Duplicate 50-μl aliquots were taken at various times after addition of 0.1 M KCl to G-actin (0.17 mg/ml in Buffer II) and subjected to centrifugation at 150,000 *g* (ave) for 5–7 min in an airfuge (Beckman Instruments, Inc. Palo Alto, CA). The amount of actin remaining unsedimented after centrifugation was determined by mixing 20 μl of supernatant with 2.0 ml of filtered Bradford reagent (4) and reading absorbance in a plastic cuvette at 595 nm. Actin concentration was determined by extrapolation from a standard curve of known G-actin concentrations. By this method, as little as 10 μg/ml actin in 20 μl of solution could be accurately quantitated. Control experiments on fully assembled F-actin solutions (0.5 mg/ml in Buffer II) demonstrated that 80–90% of the actin filaments were sedimented out of solution after 5 min of centrifugation, and complete sedimentation occurred

within 20 min. Percent assembly of actin was calculated from the formula $[(C_T - C_S)/(C_T - C_A)] \times 100$, where C_T equals total actin, C_S equals actin in the supernatant, and C_A equals the critical actin concentration.

Materials

Triethanolamine buffers were prepared with triethanolamine base (Sigma Chemical Co., St. Louis, MO) and titrated to the desired pH with HCl. TES buffers were prepared with *N*-tris (hydroxymethyl) methyl-2-aminoethane sulfonic acid (Sigma Chemical Co.) adjusted to pH with KOH. Stock solutions of 0.1 M Na_2K_2ATP were prepared by titration of Na_2ATP (Sigma Chemical Co.) to pH 7.0 with KOH. Stock solutions of ATP were stored at −20°. The pH of all buffers was determined at the experimental temperature.

RESULTS

Identification and Characterization of KCl Monomer

UV DIFFERENCE SPECTRUM OF KCL-MONOMER: In view of the initial observation by Rich and Estes (23) that unassembled G-actin incubated with 0.1 M KCl exhibits an identical behavior toward proteolytic enzymes as F-actin, one might expect the spectral appearance of a distinct monomeric actin species in the presence of KCl. Indeed, ultraviolet difference spectra of critical concentrations of both *Dictyostelium* and muscle actin at 25°C reveal the presence of an actin form that is conformationally distinct from either G-actin or F-actin (Fig. 1). We designate this species KCl-monomer although there is no evidence for any conformational difference among KCl-monomer, the F-monomer of Rich and Estes (23), or G*-actin recently observed by Rouayrenc and Travers (24). The KCl-monomer difference spectrum is characterized by a negative absorbance maximum at 212–215 nm with a slight shoulder at 220 nm. Spectra appeared stable over long periods of incubation (8 h at 25°C). Identical spectra were obtained for actin incubated in KF, indicating that the nature of the anion is not critical. The absorbance at 212 nm is equivalent to a 4% decrease of the total absorbance of G-actin (data not shown). No differences between skeletal muscle actin and *Dictyostelium* actin were detected.

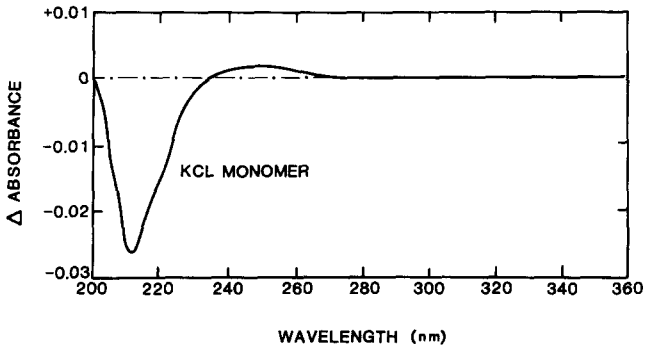

FIGURE 1 KCl-monomer UV difference spectrum. Baseline difference spectra of *Dictyostelium* G-actin (-·-·-) were taken in divided cuvettes. The KCl-monomer difference spectrum (——) was obtained after addition of buffered KCl (to 0.1 M) to 50 μg/ml G-actin (-·-·-), as described in Materials and Methods.

DEPENDENCE OF KCL-MONOMER ABSORBANCE ON ACTIN CONCENTRATION: Because the short wavelength UV region is subject to artifactual generation of signals due to light scattering by actin filaments, solution turbidities, and submicroscopic crystalline or aggregated particles, it was essential to determine the 210- to 220-nm absorbance dependence on actin concentration. The Beer's law relationship between absorbance at 215 nm and actin concentration (Fig. 2*A*) indicates that the observed spectral band is not due to light scattering but reflects a change in the molar absorbancy of the actin molecule as a result of the presence of KCl.

DEPENDENCE OF KCL-MONOMER FORMATION ON KCL CONCENTRATION: Since the difference spectrum is a measure of KCl-monomer concentration, the extent of conversion of G-actin to KCl-monomer as a function of KCl concentration could be determined (Fig. 2*B*). When a subcritical concentration of G-actin (45 μg/ml) was incubated with increasing concentrations of KCl, a slightly sigmoidal saturation curve was obtained. Saturation occurred at 0.2–0.3 M KCl which was taken as complete conversion of G-actin to KCl-monomer.

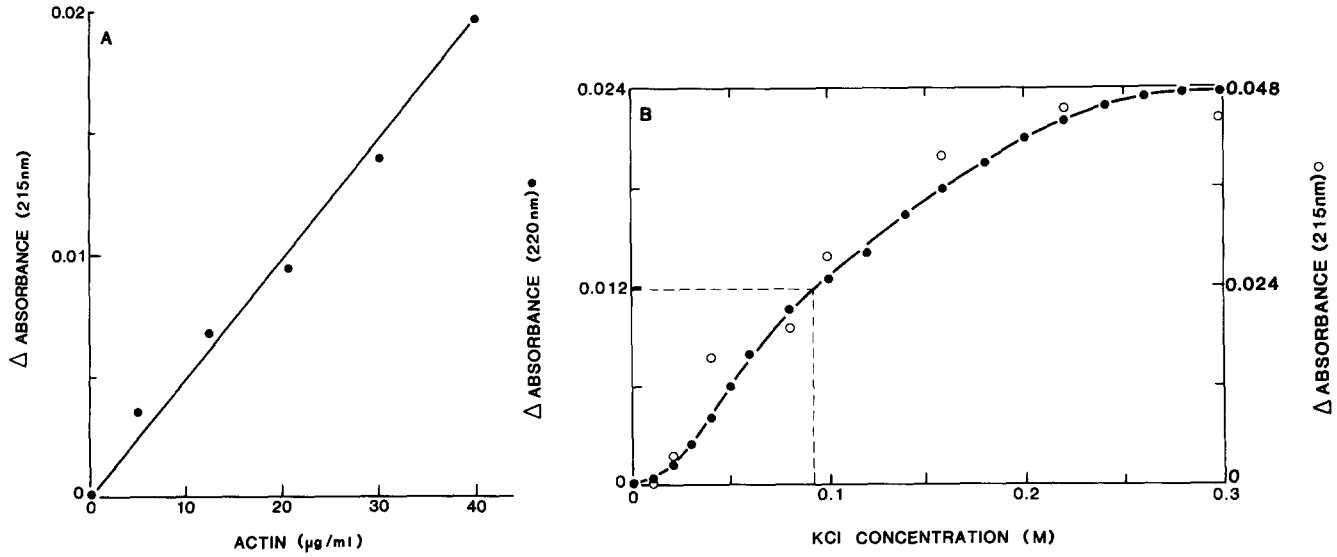

FIGURE 2 (*A*) Dependence of KCl-monomer absorbance on actin concentration. Increasing concentrations of *Dictyostelium* G-actin were incubated with 0.1 M KCl for 2–3 h at 25°C and absorbance differences at 215 nm plotted versus G-actin concentration. (*B*) Dependence of KCl-monomer formation on KCl concentration. *Dictyostelium* G-actin (45 μg/ml) was incubated with increasing concentrations of KCl at 25°C. Saturation curves were obtained at both 215 nm (○) and 220 nm (●), since 215 nm provided maximum sensitivity while spectra at 220 nm displayed a minimum of background spectral noise.

50% conversion of G-actin to KCl-monomer occurred at ~90 mM KCl. Viscometry and ΔOD_{232} determinations indicated that filament formation had not occurred during incubation with KCl. That the curve demonstrates saturation behavior provides additional evidence that the observed difference spectrum is due to KCl monomer formation and is not artifactually generated by light scattering from added KCl or absorption due to interaction of KCl with a component of the buffer.

MOLECULAR WEIGHT: Dimers or higher oligomers are not generated by conversion of G-actin to KCl-monomer. When KCl-monomer that had been observed spectrally was chromatographed over G-150 Sephadex equilibrated with 0.1 M KCl, all protein eluted entirely in the 40,000- to 45,000-dalton fractions (Fig. 3).

NUCLEOTIDE BINDING: By Scatchard plot analysis, the affinity constant (K_a) of ATP for *Dictyostelium* G-actin is 5×10^6 M^{-1} compared to 1.5×10^7 M^{-1} for KCl-monomer (Fig. 4). 1 mole of ATP is bound per mole of actin monomer in each case. Assays for the release of $^{32}P_i$ (See Materials and Methods) during conversion of G-actin to KCl-monomer and during equilibrium dialysis demonstrated that ATP was not hydrolyzed during conversion to KCl-monomer nor during incubation of KCl-monomer in high salt (<0.05 mol ATP/h per mole actin).

Assembly Properties of KCl-monomer

Evidence for the role of KCl-monomer as an intermediate in the polymerization process is indicated in Fig. 5. When G-actin at greater than critical concentration was mixed with 0.1 M KCl and immediately subjected to difference spectral analysis at 25°C against G-actin of identical concentration, the KCl monomer spectrum was immediately observed. However, as assembly occurred, the initial KCl-monomer spectrum was gradually replaced by the familiar F-actin spectrum (Fig. 5). The same spectral shift was observed if assembly was initiated by $MgCl_2$. When 1 mM Mg^{2+} was added to KCl-monomer (50 μg/ml in 0.1 M KCl), the critical actin concentration dropped from 50 μg/ml to ~10 μg/ml, and assembly was initiated. Successive spectral scans taken after addition of Mg^{2+} revealed the occurrence of actin assembly: (*a*) 0–5 min after Mg^{2+}

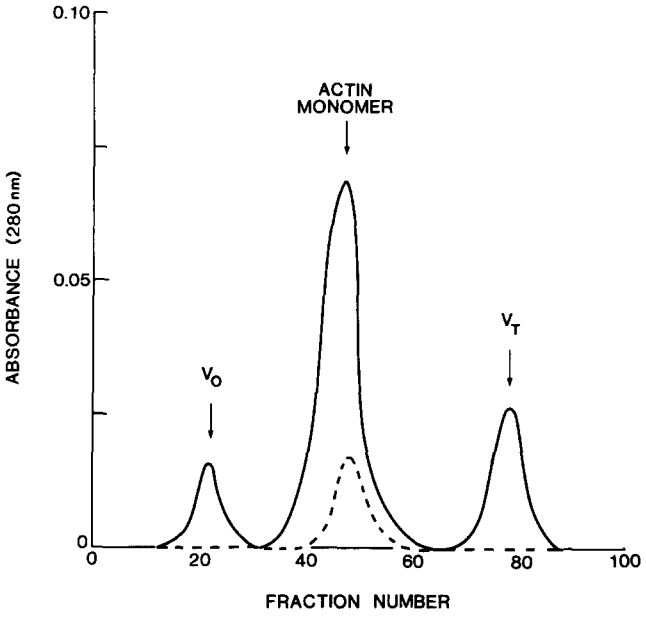

FIGURE 3 G-150 Sephadex chromatography of KCl-monomer. Depolymerized *Dictyostelium* actin (1 mg/ml) in Buffer I was eluted from G-150 Sephadex to obtain oligomer-free actin monomers for UV difference spectral determinations (——). Undepolymerized actin eluted at V_o, and excess free nucleotide eluted at V_T. Monomeric actin was pooled, diluted to 50 μg/ml with Buffer I, and UV difference spectra of KCl monomer were obtained upon addition of KCl to 0.1 M. The resulting KCl-monomer actin (50 μg/ml) was subsequently rechromatographed through the same column which had been reequilibrated with Buffer I containing 0.1 M KCl (- - -). KCl-monomer from either *Dictyostelium* or muscle actin eluted as a single peak in the position of monomeric G-actin.

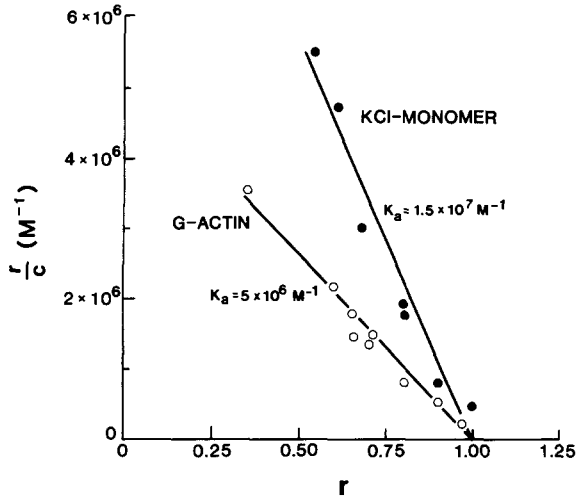

FIGURE 4 Affinity of ATP for G-actin and KCl-monomer. Equilibrium dialysis experiments were performed at 4°C using column purified *Dictyostelium* G-actin (1.2 μM) with (●) or without (○) 0.1 M KCl. All actin samples included in the Scatchard analysis demonstrated >90% assembly competency after equilibrium dialysis. Affinity constants were determined from the slope of each curve, and mol ATP_{bound}/mol actin by extrapolation to the *r* axis. $r = [ATP]_{bound}/[actin]$; $c = [ATP]_{free}$.

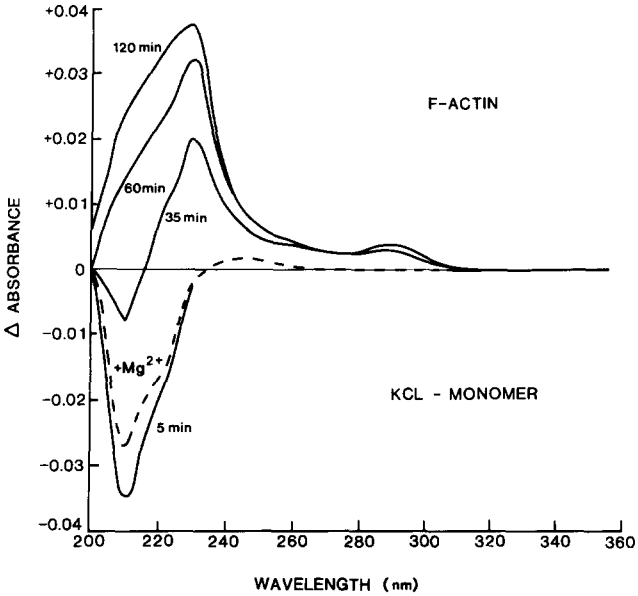

FIGURE 5 UV difference spectra of assembling KCl-monomer. KCl (to 0.1 M) was added to 100 μg/ml *Dictyostelium* G-actin in a divided cuvette and difference spectra taken intermittently over a 2-h period (——). In a separate experiment, 1 mM $MgCl_2$ was added to a sample of KCl-monomer at 50 μg/ml (- - -). Baseline (Δ A = 0) is of G-actin versus G-actin at 25°C.

addition, the KCl-monomer difference spectrum was observed (Fig 5, dashed line). (*b*) the KCl-monomer spectrum was gradually transformed into the classical F-actin spectrum with the appearance of positive absorbance maxima at 280–290 nm and 232 nm (data not shown).

We conclude that polymerization in the presence of KCl or KCl + Mg^{2+} occurs in two distinct stages, conversion of G-actin to KCl-monomer, followed by incorporation of monomer into filaments. KCl-monomer therefore appears as an intermediate in the assembly process.

ASSEMBLY KINETICS: The kinetics of K^+-triggered actin assembly vs. K^+ + Mg^{2+}-triggered assembly were directly compared by viscometry, ΔOD_{232}, rapid sedimentation, and ATP hydrolysis. The critical actin concentration measured by viscosity was 10 μg/ml for either skeletal muscle or *Dictyostelium* actin assembled with 0.1 M KCl + 0.2 mM $MgCl_2$ compared to 50 μg/ml for actin assembled with 0.1 M KCl alone. Reduced viscosities were 15 dl/g for both types of filaments. Fig. 6*A* compares the increases in viscosity, absorbance, and ATP hydrolysis observed for identical aliquots of a single actin sample assembled with 0.1 M KCl + 0.2 mM $MgCl_2$. The assembly half-time ($t_{1/2}$) as measured by ΔOD_{232} was 1.5 min compared to 1.7 min by viscosity for an actin concentration of 0.5 mg/ml. ATP hydrolysis consistently lagged assembly, exhibiting a $t_{1/2}$ of 4.5 min. A distinct plateau of ATP hydrolysis was observed at 0.95 mole ATP hydrolyzed/mole actin monomer.

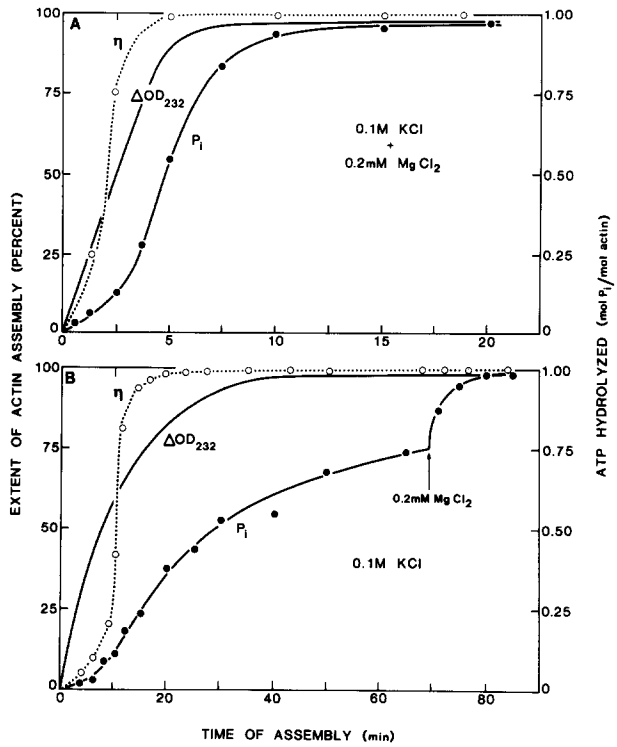

FIGURE 6 Comparative kinetics of actin assembly. (*A*) Identical aliquots of G-150 Sephadex column purified *Dictyostelium* G-actin (0.5 mg/ml) were assembled in parallel experiments by addition of 0.1 M KCl + 0.2 mM $MgCl_2$. Assembly was monitored simultaneously by viscometry (○), ΔOD_{232} (——), and hydrolysis of actin-bound [γ-^{32}P]-ATP (●). C_A = 10 μg/ml. Muscle actin demonstrated similar assembly kinetics (data not shown). (*B*) Identical aliquots of *Dictyostelium* G-actin (0.5 mg/ml) were assembled in parallel by addition of 0.1 M KCl. C_A = 50 μg/ml. Muscle actin gave similar assembly kinetics (data not shown).

By assembling 0.5 mg/ml actin with 0.1 M KCl in the absence of added divalent cations, all of the features of assembly with K^+ + Mg^{2+} were preserved but the reaction was sufficiently slowed to enable resolving important details of the polymerizations process (Fig. 6*B*). ATP hydrolysis was found to lag far behind the assembly of monomers into filaments as indicated by ΔOD_{232} or viscosity. The half-time for ATP hydrolysis was 30 min compared to 7.5 min for ΔOD_{232} or 10 min by viscosity. By the time maximal viscosity was achieved, only 25% of maximal ATP hydrolysis had occurred, and, at 50% completion of assembly as measured by either ΔOD_{232} or viscosity, only 6–8% completion of ATP hydrolysis had occurred. Addition of 0.2 mM $MgCl_2$ after completion of assembly as indicated by ΔOD_{232} or viscometry, but before completion of ATP hydrolysis, caused a rapid burst of hydrolysis to 1 mole ATP cleaved/mole actin.

Apparently, under these conditions incorporation of KCl monomers into filaments occurs without ATP hydrolysis, and divalent cations greatly accelerate hydrolysis of ATP bound to F-actin. As evidenced by either viscometry or ΔOD_{232}, ATP hydrolysis occurs significantly after the incorporation of a monomer into the filament structure. Since only 6–8% of the actin-bound ATP is hydrolyzed at 50% assembly, and since only 25% hydrolysis has occurred at the time of complete filament formation, we conclude that long filaments containing bound ATP are present in the mixture. Therefore a second intermediate (F[ATP]-actin) in the assembly process is kinetically resolved.

EFFECT OF KCl, AND $MgCl_2$ ON ASSEMBLY RATE AND ATP HYDROLYSIS: The extent of ATP hydrolysis at half-maximal assembly is independent of salt concentration, the presence or absence of Mg^{2+}, or the initial rate of assembly. When actin was assembled under various ionic conditions, and ATPase activity monitored simultaneously along with assembly by ΔOD_{232} or viscometry, the extent of ATP hydrolysis appeared constant at 7–10% of maximum after 50% completion of assembly (Fig. 7*A*). The rate of assembly, however, is highly dependent upon KCl concentration (Fig. 7*B*).

COMPARATIVE ASSEMBLY KINETICS BY VISCOMETRY, ΔOD_{232}, AND SEDIMENTATION: A critical feature revealed by polymerization induced with K^+ is the apparent discrepancy between the assembly kinetics observed by ΔOD_{232} and viscometry. To determine which method accurately reflects the appearance of filaments in the reaction mixture, we used a rapid sedimentation technique capable of pelleting 80% of the assembled actin filaments within 5 min (see Materials and Methods).

Assembly of muscle actin (0.17 mg/ml in Buffer II) by 0.1 M KCl alone was sufficiently slow to obtain reproducible sedimentation data from centrifugation. The kinetics of actin assembly by rapid sedimentation agree closely with those obtained by ΔOD_{232} but not with viscosity measurements (Fig. 8). Within the time-resolving limits of ΔOD_{232} and rapid sedimentation determinations, the incorporation of monomers into filaments did not demonstrate an observable lag phase. A pronounced lag period, followed by rapid assembly, and abrupt cessation of polymerization was observed only by viscometry. Lag periods were observed by viscometry when concentrations of 25, 50, and 100 mM KCl or 100 mM KCl + 0.2 mM $MgCl_2$ were used to initiate assembly, provided that sufficiently low concentrations of actin were used to slow the reaction and thereby enable time resolution of the viscometry curves. However, lag phases were not detected at the same actin and salt concentrations when assembly was monitored by ΔOD_{232} and

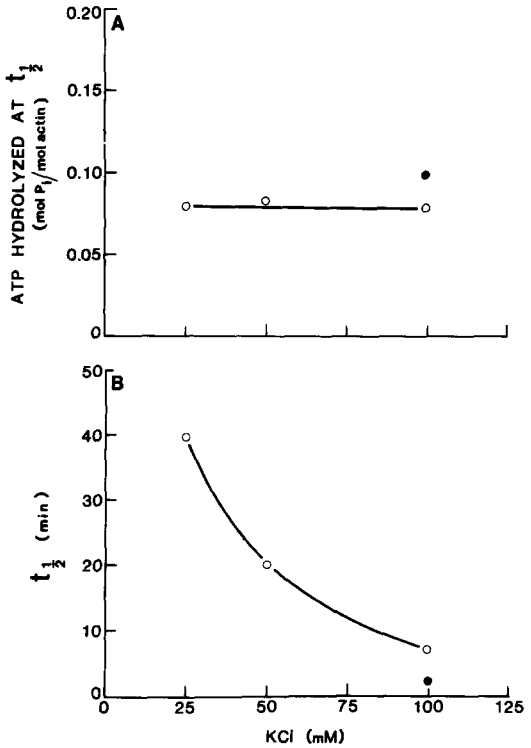

FIGURE 7 Effect of KCl concentration on ATP hydrolysis and assembly rate. KCl was added to *Dictyostelium* G-actin (0.5 mg/ml) and assembly monitored by ΔOD_{232} and viscometry. The half-times for assembly by ΔOD_{232} and viscometry were similar, as in Fig. 6. (*A*) Extent of ATP hydrolysis at 50% maximum assembly ($t_{1/2}$) is plotted as a function of KCl concentration (○). Data for actin assembled with 0.1 M KCl + 0.2 mM $MgCl_2$ are also given (●). (*B*) The half-time ($t_{1/2}$) for actin assembly is plotted as a function of KCl concentration (○) and for 0.1 M KCl + 0.2 mM $MgCl_2$ (●).

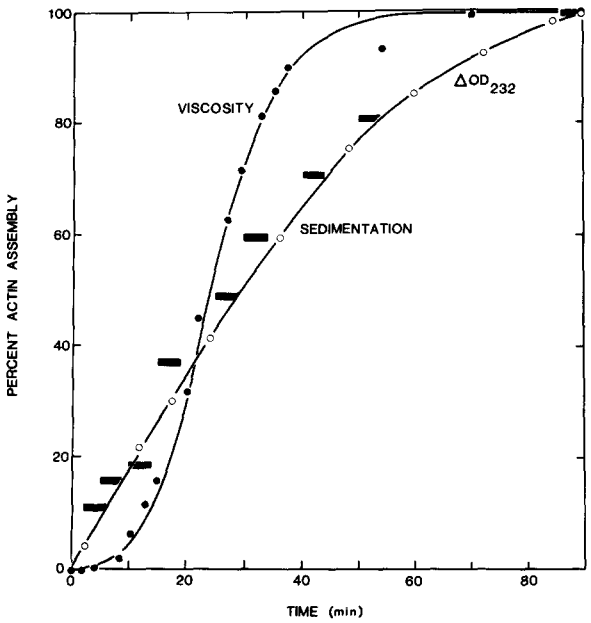

FIGURE 8 Kinetics of actin assembly by viscometry, ΔOD_{232}, and rapid sedimentation. Identical aliquots of column purified rabbit skeletal muscle G-actin (0.17 mg/ml) were assembled by addition of 0.1 M KCl, and assembly followed in parallel experiments by *viscometry* (●), ΔOD_{232} (○), and rapid *sedimentation* (▬). Data are the average of three different experiments. Data are normalized to 100% completion of assembly (see Materials and Methods).

rapid sedimentation. Although assembly kinetics appear strikingly different by ΔOD_{232} or sedimentation vs. viscometry, the times required for half-maximal assembly ($t_{1/2}$) are nearly equivalent for each technique.

DISCUSSION

The purpose of these studies was to gain insight into the biochemical processes that occur when actin is assembled by physiological concentrations of K^+. We conclude that:

(*a*) An actin species which is neither G- nor F-actin is observed spectroscopically in actin solutions incubated with high concentrations of KCl. The conformer has been termed KCl-monomer. Although not proven, this KCl-mononer observed by difference spectroscopy in the 215-nm range is likely to be the same species observed by Rich and Estes (23) by protease sensitivity, and by Rouayrenc and Travers (24) by difference spectroscopy in the 275-nm range. F-monomer (23), G*-actin (24) and the KCl-monomer described here all appear to be monomeric and contain bound ATP.

(*b*) KCl-monomer is observed after addition of salt and disappears during the course of assembly into filaments. We interpret this as indicative of an intermediate position for KCl-monomer in the assembly process.

(*c*) ATP hydrolysis lags far behind the assembly of actin monomers into filaments when actin is assembled by K^+ alone or $K^+ + Mg^{2+}$. ATP hydrolysis is therefore considered to be decoupled from the insertion of monomer actin into a growing filament.

These results indicate the following reaction sequence for the assembly of actin:

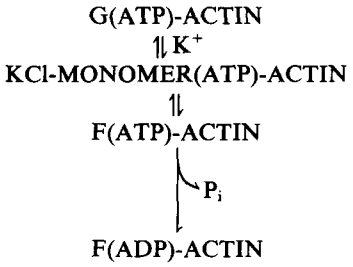

Two intermediate species between the classically recognized G-actin and F-actin participate in the assembly process when physiological concentrations of KCl are present; KCl-monomer and filaments containing bound ATP. Irreversible hydrolysis of filament-bound ATP produces the final F(ADP)-actin product.

The observation of decoupled ATP hydrolysis affords a demonstration of the order of events during filament formation. Cooke (9) observed that the rate of assembly did not depend on the concentration of P_i and concluded that dephosphorylation was not coupled to the initial polymerization step. Moreover, actin assembly proceeded at the same rate when AMP·PNP instead of ATP was bound to G-actin. That result was consistent with previous hypotheses that ATP binding but not hydrolysis provided the energy for protein interactions (3, 20). Here we provide a direct demonstration that ATP hydrolysis occurs subsequent to monomer incorporation into filaments (Fig. 6). Because 50% assembly completion is constantly associated with ~8% ATP hydrolysis regardless of salt condition or assembly rate (Fig. 7), we suggest that hydrolysis of filament-

bound ATP is triggered after formation of extensive stretches of F(ATP)-actin. Whether hydrolysis occurs at random along the filament length or sequentially from one filament end to the other is unknown. To initiate the ATPase assay, the actin samples are plunged into ice-cold perchloric acid, a method known to quickly release all bound nucleotide from actin (30). We conclude, therefore, that the observed lag in appearance of P_i corresponds to a lag in actin-bound ATP hydrolysis and not a lag in the release of P_i from the actin filament.

The kinetics of actin polymerization have been followed by a variety of methods. Kasai et al. (14) first studied the kinetics of polymerization by viscometry, and found it to follow a sigmoidal curve. A rate-limiting initial nucleation step involving highly cooperative binding of several monomers into a filament nucleus was postulated (13, 14, 22). By ΔOD_{232}, however, Cooke noted that polymerization followed a simple exponential for G-actin containing ATP, ADP, or AMPPNP but attributed the observed kinetics to possible contamination of G-actin with nuclei (9). Higashi and Oosawa (10) have reported exponential rises for G-ADP-actin assembly by both ΔOD_{232} and birefringence. Furthermore, Taylor et al. (31) have observed a hyperbolic assembly curve by fluorescence energy transfer. We also observed simple exponential kinetics using ΔOD_{232} and sedimentation. In parallel experiments with identical actin samples a pronounced lag phase in the kinetics of assembly was observed only by viscometry. This suggests that viscosity is an insensitive method for determining the initial time course of polymerization. Since the intrinsic viscosity $[\eta]$ for long prolate ellipsoids or a rigid string of spherical beads is proportional to $(\text{length})^{1.8}$ (16, 26), the difference in viscosity between a 4-μm actin filament and a 0.2-μm filament is very large (~230-fold). Therefore, viscometers sensitive to long filament length at full assembly may fail to detect the formation of oligomers during the initial stages of actin polymerization. Furthermore, the high shear Ostwald viscometers traditionally used to monitor assembly may break filaments repeatedly during the course of assembly determinations. The time resolution of ΔOD_{232} or sedimentation determinations in these experiments is not fast enough to discriminate between strict hyperbolic kinetics and a slight lag period during initiation of assembly. Therefore, we cannot determine whether assembly is noncooperative or exhibits a low level of cooperativity.

In summary, by studying the assembly reaction in the presence of K^+, it appears that actin polymerization is controlled by a conformational shift which immediately precedes assembly. Incorporation of ATP-containing monomers into filaments is followed by dephosphorylation of filament-bound ATP to yield F(ADP)-actin.

This investigation was supported by a grant from the National Institutes of Health (#GM 25240) to J. A. Spudich, and a Damon Runyon-Walter Winchell Postdoctoral Fellowship to J. D. Pardee.

REFERENCES

1. Asakura, S., K. Motta, N. Imai, T. Ooi, and F. Oosawa. 1958. *Conference on the Chemistry of Muscular Contraction*. Igaku Shoin, Ltd., Tokyo. 57–65.
2. Bárány, M., N. A. Bird, and J. Molnar. 1954. Über die reaktion aktin und zweiwertigen kationen. *Acta Physiol. Acad. Sci. Hung.* 5:63–78.
3. Boyer, P. D., R. L. Cross, and W. Momsen. 1973. A new concept for energy coupling in oxidative phosphorylation based on a molecular explanation of the oxygen exchange reactions. *Proc. Natl. Acad. Sci. U. S. A.* 70:2837–2839.
4. Bradford, M. M. 1976. A rapid and sensitive method for the quantitation of μg quantities of protein utilizing the principle of protein-dye binding. *Anal. Biochem.* 72:248–254.
5. Bray, D., and C. Thomas. 1976. Unpolymerized actin in fibroblasts and brain. *J. Mol. Biol.* 105:527–544.
6. Chamberlin, M. J., and J. Ring. 1972. Studies of the binding of *Escherichia coli* RNA polymerase to DNA. *J. Mol. Biol.* 70:221–237.
7. Clarke, M., and J. A. Spudich. 1974. Biochemical and structural studies of actomyosin-like proteins from nonmuscle cells. *J. Mol. Biol.* 86:209–222.
8. Conway, E. J. 1975. Nature and significance of concentration relations of potassium and sodium ions in skeletal muscle. *Physiol. Rev.* 37:84–132.
9. Cooke, R. 1975. The role of the bound nucleotide in the polymerization of actin. *Biochemistry.* 14:3250–3256.
10. Higashi, S., and F. Oosawa. 1965. Conformational changes associated with polymerization and nucleotide binding in actin molecules. *J. Mol. Biol.* 12:843–865.
11. Hodgkin, A. L. 1958. Ionic movements and electrical activity in giant nerve fibres. *Proc. R. Soc. Lond. B Biol. Sci.* 148:1–37.
12. Houk, T. W., Jr., and K. Ue. 1974. The measurement of actin concentration in solution: a comparison of methods. *Anal. Biochem.* 62:66–74.
13. Kasai, M. 1969. Thermodynamical aspect of G-F transformations of actin. *Biochem. Biophys. Acta.* 180:399–409.
14. Kasai, M., S. Asakura. and F. Oosawa. 1962. The cooperative nature of G-F transformation of actin. *Biochem. Biophys. Acta.* 57:27–31.
15. Kawamura, M., and K. Maruyama. 1970. Polymorphism of F-actin. I. Three forms of paracrystals. *J. Biochem. (Tokyo).* 68:885–899.
16. Kirkwood, J. G., and P. L. Auer. 1951. The visco-elastic properties of solutions of rodlike macromolecules. *J. Chem. Phys.* 19:281–283.
17. Lindberg, U., L. Carlsson, F. Markey, and L. E. Nyström. 1979. Methods and Achievements in Experimental Biology, Vol. 8. G. Gabbiani, editor. S. Karger, Federal Rebublic of Germany. 143–170.
18. Martonosi, A., C. M. Molino, and J. Gergely. 1964. The binding of divalent cations to actin. *J. Biol. Chem.* 239:1057–1064.
19. Mommaerts, W. F. H. M. 1952. The molecular transformations of actin. I. Globular actin. *J. Biol. Chem.* 198:459–467.
20. Morales, M. F. and J. Botts. 1952. A model for the elementary process in muscle action. *Arch. Biochem. Biophys.* 37:283–300.
21. Oosawa, F., S. Asakura, K. Hotta, N. Imai, and T. Ooi. 1959. G-F transformation of actin as a fibrous condensation. *J. Polym. Sci. Part D Macromol. Rev.* 37:323–336.
22. Oosawa, F., and M. Kasai. 1971. Actin, *In*: *Subunits in Biological Systems, Part A, Vol. 5.* S. N. Timasheff and G. D. Fasman, editors. Biological Macromolecules Series, M. Dekker, NY. 292.
23. Rich, S. A., and J. E. Estes. 1976. Detection of conformational changes in actin by proteolytic digestion: evidence for a new monomeric species. *J. Mol. Biol.* 104:777–792.
24. Rouayrenc, J., and F. Travers. 1981. The first step in the polymerization of actin. *Eur. J. Biochem.* 116:73–77.
25. Scatchard, G. 1949. The attractions of proteins for small molecules and ions. *Ann. N. Y. Acad. Sci.* 51:660–672.
26. Simha, R. 1940. The influence of brownian movement on the viscosity of solutions. *J. Phys. Chem.* 44:25–34.
27. Spudich, J. A., and S. Watt. 1971. The regulation of rabbit skeletal muscle contraction. *J. Biol. Chem.* 246:4866–4871.
28. Straub, F. B. 1942. Actin. *In*: *Studies from the Institute of Medical Chemistry, University of Szeged,* 2:3–15.
29. Strzelecka-Golaszewska, H., E. Prochniewicz, and W. Drabikowski. 1978. Interaction of actin with divalent cations, II. Characterization of protein-metal complexes. *Eur. J. Biochem.* 88:229–237.
30. Sugino, Y., and Y. Miyoshi. 1964. The specific precipitation of orthophosphate and some biochemical applications. *J. Biol. Chem.* 239:2360–2364.
31. Taylor, D. L., J. Reidler, J. A. Spudich, and L. Stryer. 1981. Detection of actin assembly by fluorescence energy transfer. *J. Cell Biol.* 89:362–367.
32. Uyemura, D. G., S. S. Brown, and J. A. Spudich. 1978. Biochemical and structural characterization of actin from *Dictyostelium discoideum*. *J. Biol. Chem.* 253:9088–9096.
33. West, J. J., B. Nagy, and J. Gergely. 1967. The effect of EDTA on spectral properties of ATP-, ADP-, and ITP-G-actin. *Biochem. Biophys. Res. Commun.* 29:611–616.